Regulation of ER-phagy by a Ypt/Rab GTPase module

Zhanna Lipatova[a], Ankur H. Shah[b], Jane J. Kim[b], Jonathan W. Mulholland[c], and Nava Segev[a]
[a]Department of Biochemistry and Molecular Genetics and [b]Department of Biological Sciences, University of Illinois at Chicago, Chicago, IL 60612; [c]Cell Sciences Imaging Facility, Beckman Center, Stanford University School of Medicine, Stanford, CA 94305

ABSTRACT **Accumulation of misfolded proteins on intracellular membranes has been implicated in neurodegenerative diseases. One cellular pathway that clears such aggregates is endoplasmic reticulum autophagy (ER-phagy), a selective autophagy pathway that delivers excess ER to the lysosome for degradation. Not much is known about the regulation of ER-phagy. The conserved Ypt/Rab GTPases regulate all membrane trafficking events in eukaryotic cells. We recently showed that a Ypt module, consisting of Ypt1 and autophagy-specific upstream activator and downstream effector, regulates the onset of selective autophagy in yeast. Here we show that this module acts at the ER. Autophagy-specific mutations in its components cause accumulation of excess membrane proteins on aberrant ER structures and induction of ER stress. This accumulation is due to a block in transport of these membranes to the lysosome, where they are normally cleared. These findings establish a role for an autophagy-specific Ypt1 module in the regulation of ER-phagy. Moreover, because Ypt1 is a known key regulator of ER-to-Golgi transport, these findings establish a second role for Ypt1 at the ER. We therefore propose that individual Ypt/Rabs, in the context of distinct modules, can coordinate alternative trafficking steps from one cellular compartment to different destinations.**

Monitoring Editor
Benjamin S. Glick
University of Chicago

Received: May 21, 2013
Revised: Jul 24, 2013
Accepted: Jul 30, 2013

INTRODUCTION

At the cellular level, neurodegenerative diseases are associated with accumulation of aggregated proteins termed neurodegenerative-related (NDR) proteins, such as α-synuclein in Parkinson, amyloid precursor protein in Alzheimer, and PrP in prion-related diseases (Uversky *et al.*, 2009). The cause of the toxicity of these aggregates is not well understood. One common feature of NDR proteins is that they are all integral or membrane-associated proteins (Fantini and Yahi, 2010). On synthesis, all integral membrane proteins are inserted into the endoplasmic reticulum (ER), a membrane network that spans the whole cell. Exit of membrane proteins from the ER to other cellular compartments depends on their proper folding, a process that is not 100% efficient, yielding a subset of misfolded proteins. One mechanism for clearance of misfolded proteins is shuttling to the lysosome for degradation via the autophagy pathway (Schroder, 2008; Vembar and Brodsky, 2008).

Transport of membranes and proteins through cellular trafficking pathways connects membrane-bound intracellular compartments with the plasma membrane (PM) and the cell milieu. In the exocytic pathway, transport flows from the ER through the Golgi toward the PM, whereas in the endocytic pathway, transport flows from the PM through endosomes toward the lysosome. In addition, selective and nonselective autophagic pathways deliver proteins and membranes, from various intracellular compartments or bulk cytoplasm, for degradation in the lysosome. ER-phagy is a selective autophagy pathway, which targets aberrant ER (Bernales *et al.*, 2007; Deegan *et al.*, 2013). Misfolded or excess proteins at the ER can be shuttled for degradation either to the proteosome or, via the ER-phagy pathway, to the lysosome (Bernales *et al.*, 2007; Vembar and Brodsky, 2008). Disruption of this shuttling and subsequent accumulation of misfolded proteins at the ER results in

This article was published online ahead of print in MBoC in Press (http://www.molbiolcell.org/cgi/doi/10.1091/mbc.E13-05-0269) on August 7, 2013.

Address correspondence to: Nava Segev (nava@uic.edu).

Abbreviations used: EM, electron microscopy; ER, endoplasmic reticulum; GEF, guanine-nucleotide exchange factor; GFP, green fluorescent protein; PAS, pre-autophagosomal structure; PM, plasma membrane; UPR, unfolded protein response; YFP, yellow fluorescent protein.

Supplemental Material can be found at:
http://www.molbiolcell.org/content/suppl/2013/08/05/mbc.E13-05-0269v1.DC1

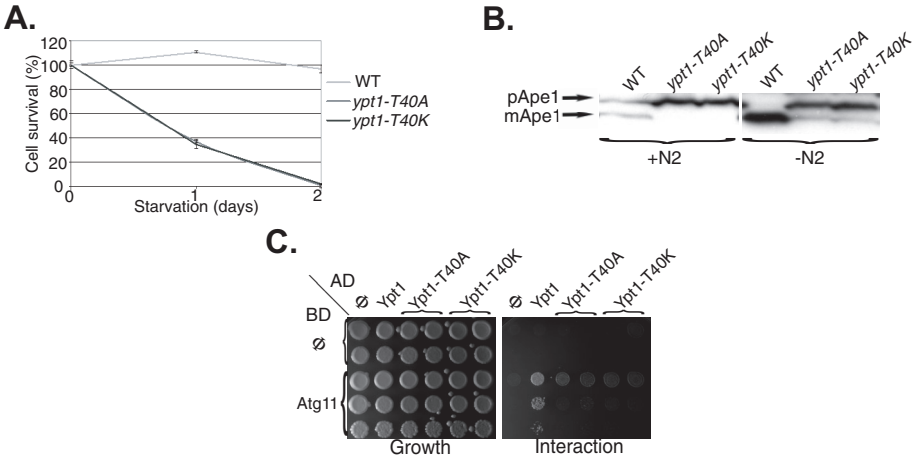

FIGURE 1: The *YPT1-T40A* mutation, like *YPT1-T40K*, confers autophagy and Atg11-binding defects. (A) Similar to *ypt1-T40K* (*ypt1-1*), *ypt1-T40A* mutant cells are defective in nonselective autophagy. Cells were deleted for the *YPT1* gene on the chromosome and express one of the following alleles of *YPT1* from a *CEN* plasmid under its own promoter and terminator: *YPT1* (WT), *ypt1-T40K*, or *ypt1-T40A*. The viability of the cells was determined before and after a shift to medium without nitrogen. Shown is percentage cell survival after the shift (100% before the shift); error bars, SD). Whereas wild-type cells remained viable, both *ypt1* mutant strains lost their viability after 2 d of nitrogen starvation. (B) Similar to *ypt1-T40K* (*ypt1-1*), *ypt1-T40A* mutant cells are defective in CVT. Processing of Ape1 in the three strains (as in A) was determined using immunoblot analysis with anti-Ape1 antibodies before and 4 h after a shift to medium without nitrogen. Whereas wild-type cells process pApe1 to mApe1 (mature), both *ypt1-T40K* and *ypt1-T40A* mutant cells are defective in this processing. (C) The Ypt1-T40A mutant protein, like Ypt1-T40K, does not interact with Atg11 in the yeast two-hybrid (Y2H) assay. Interaction was determined using a mating assay with two Y2H plasmids. Activation domain (AD): Φ, Ypt1, Ypt1-T40K, and Ypt1-T40A (left to right). Binding domain (BD): Φ or Atg11 (top to bottom). Growth of the diploids carrying the two plasmids is shown on SD-Ura-Leu (left), and interaction is shown on SD-Ura-Leu-His (right). Whereas wild-type Ypt1 interacts with Atg11, both mutant proteins are defective in this interaction. Results represent at least two independent experiments.

ER stress and induction of the unfolded protein response (UPR; Schroder, 2008).

All types of autophagy start with the formation of the pre-autophagosomal structure (PAS; Nakatogawa *et al.*, 2009; Yang and Klionsky, 2009). The PAS is required for the formation of the double-membrane autophagosome, which engulfs parts of the cytoplasm and then fuses with the lysosome. Much research has been done on elucidating the signaling pathways that induce or suppress autophagy (He and Klionsky, 2009; Wang and Levine, 2010) and identifying autophagy-specific machinery components (Nakatogawa *et al.*, 2009; Yang and Klionsky, 2009). The current consensus is that the autophagosomal membrane originates from the ER and other cellular compartments, such as mitochondria or the Golgi–endosomal system (Yang and Klionsky, 2009; Tooze and Yoshimori, 2010). It is not clear, however, how autophagy machinery intersects with membrane trafficking machinery to generate the autophagosome (Rubinsztein *et al.*, 2012).

Ypt/Rabs are conserved monomeric GTPases that regulate trafficking between cellular compartments. These GTPases are stimulated by guanine-nucleotide exchange factors (GEFs) to recruit multiple effectors, which mediate all vesicular transport events, from vesicle formation to their targeting and fusion (Segev, 2001a,b; Stenmark, 2009). Recently Ypt/Rab GTPases have also emerged as candidates for coordination of individual transport steps in the same pathway (Segev, 2011). Here we address the question of whether Ypt/Rabs can coordinate distinct intracellular trafficking pathways and, specifically, regulate the intersection between the exocytic and autophagic pathways.

In yeast, Ypt1 is required for ER-to-Golgi transport (Segev *et al.*, 1988; Jedd *et al.*, 1995) and autophagy (Segev and Botstein, 1987; Lynch-Day *et al.*, 2010). The Ypt31/32 functional pair also plays a role in two transport steps: Golgi to PM and endosomes to Golgi (Jedd *et al.*, 1997; Chen *et al.*, 2005). One possible scenario is that a single Ypt can play different roles in distinct locations. Evidence in favor of this model has been presented for Ypt1, which in addition to its established roles in ER-to-Golgi transport and autophagy, was suggested to play a role in endosome-to-Golgi transport (Sclafani *et al.*, 2010). An alternative explanation is that Ypt1 has different roles at a single location. Our new data favor the latter model, which may establish a new paradigm for the action of Ypt/Rab GTPases.

The GEF for Ypt1 and Ypt31/32 is the multisubunit modular TRAPP complex, which is found in at least three configurations. TRAPPI acts as a GEF for Ypt1 (Jones *et al.*, 2000; Wang *et al.*, 2000) and is required for ER-to-Golgi transport (Sacher *et al.*, 1998). TRAPPIII, which contains the TRAPPI subunits plus Trs85, acts as a Ypt1 GEF in autophagy (Lynch-Day *et al.*, 2010). TRAPPII, which contains Trs120 and Trs130 in addition to TRAPPI subunits, acts at the *trans*-Golgi (Sacher *et al.*, 2001). The GEF specificity of TRAPPII has differing reports (Morozova *et al.*, 2006; Cai *et al.*, 2008).

We recently showed that a Ypt/Rab module consisting of the autophagy-specific Trs85-contaning TRAPPIII as a GEF, Ypt1, and Atg11 as an effector (Trs85-Ypt1-Atg11) is required for PAS formation (Lipatova *et al.*, 2012). It was not clear, however, from which compartment this Ypt module shuttles membranes and proteins to the autophagic pathway. Here we show that the Trs85-Ypt1-Atg11 module functions at the ER to clear excess and/or misfolded proteins. Our results establish that Ypt1 acts at the ER to coordinate two different transport steps: ER-phagy and ER-to-Golgi transport. Because all of the players are conserved from yeast to humans, elucidation of such coordination is pertinent to tackling neurodegenerative disorders.

RESULTS

Accumulation of membrane proteins in aberrant ER of *ypt1* mutant cells

Ypt1 is essential for both ER-to-Golgi transport and autophagy (Segev and Botstein, 1987; Segev *et al.*, 1988; Jedd *et al.*, 1995; Lynch-Day *et al.*, 2010; Lipatova *et al.*, 2012). We hypothesized that, like cargo-containing vesicles destined for the Golgi apparatus, Ypt1-mediated flow of cellular components to autophagy also originates from the ER. To test this idea, we used two *ypt1* mutations that do not exhibit an ER-to-Golgi transport defect but confer an autophagy-specific block: *ypt1-T40K* (*ypt1-1*) and *ypt1-T40A*.

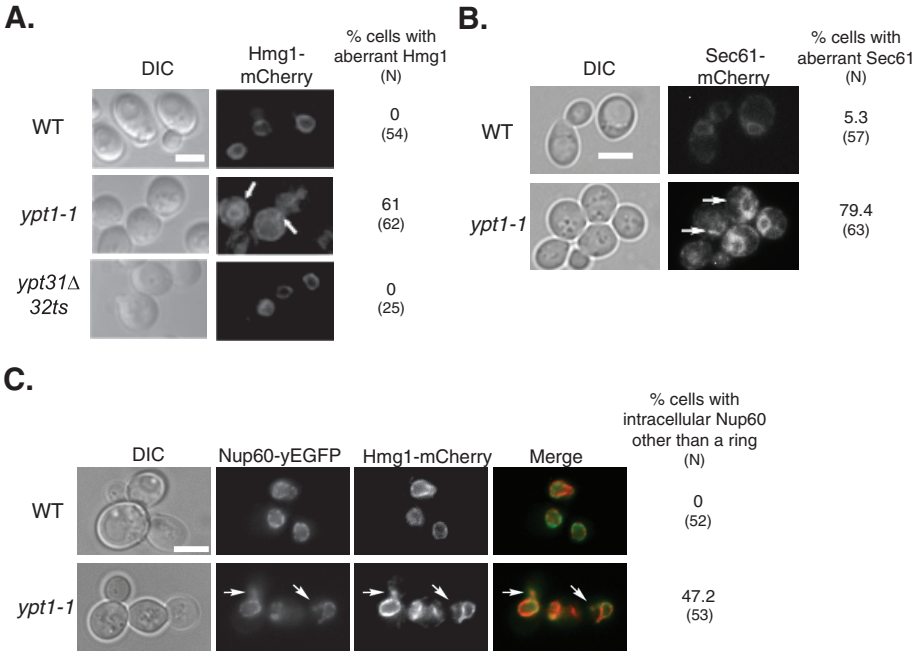

FIGURE 2: Excess ER accumulates in *ypt1-1* mutant cells expressing fluorescently tagged ER proteins. (A) Excess ER accumulates in *ypt1-1* mutant cells expressing Hmg1-mCherry. The ER protein Hmg1 was tagged on the chromosome with mCherry in wild-type and *ypt1-1* and *ypt31Δ/32ts* mutant cells. Cells were visualized by live-cell fluorescence microscopy. Left to right, differential interference contrast (DIC), mCherry, and percentage of cells with aberrant Hmg1 structures (*N*, number of cells visualized). In wild-type and *ypt31Δ/32ts* mutant cells, mCherry-tagged Hmg1 localizes to rings around nuclei, a typical ER staining pattern (Huh *et al.*, 2003). On the other hand, excess ER structures accumulate in the majority of *ypt1-1* mutant cells. (B) Excess ER accumulates in *ypt1-1* mutant cells expressing Sec61-mCherry. Sec61 was tagged on the chromosome with mCherry in wild-type and *ypt1-1* mutant cells. Cells were visualized by live-cell fluorescence microscopy. Left to right, DIC, mCherry, and percentage of cells with aberrant Sec61 structures (*N*, number of cells visualized). In wild-type cells, mCherry-tagged Sec61 localizes to rings around nuclei and underneath the PM, as previously seen for Sec61-GFP (Huh *et al.*, 2003). In addition, excess ER structures accumulate in the majority of *ypt1-1* mutant cells. (C) Excess ER accumulates in *ypt1-1* mutant cells expressing Nup60–yeast enhanced GFP (yEGFP) and Hmg1-mCherry. The nuclear pore protein Nup60 was tagged on the chromosome with yEGFP in wild type and *ypt1-1* mutant cells expressing Hmg1-mCherry. Cells were visualized by live-cell fluorescence microscopy. Left to right, DIC, GFP, mCherry, merge, percentage of cells with Nup60 other than the ring (*N*, number of cells visualized). In wild-type cells, Nup60-GFP localizes to rings around nuclei (Huh *et al.*, 2003). About half of the *ypt1-1* mutant cells (47%) contain structures other than the rings in which Nup60-GFP colocalizes with Hmg1-mCherry (92%). Arrows point to aberrant ER structures; bars, 5 μm. Results represent at least two independent experiments.

Cells expressing the *ypt1-1* mutation from the endogenous locus are sensitive to cold and, mildly, to elevated temperatures. At the permissive temperature, this mutation does not cause a vegetative growth defect or an ER-to-Golgi block (Segev and Botstein, 1987; Segev *et al.*, 1988; Jedd *et al.*, 1995). The second allele is *ypt1-T40A*, which is a substitution of the same amino acid as in the *ypt1-1* allele, T40K, but to alanine. The *ypt1-T40A* allele, when expressed from a plasmid as the sole copy of *YPT1*, does not exhibit defects in the secretory pathway (Sclafani *et al.*, 2010). To compare the two alleles, we constructed them in a *CEN* plasmid with the promoter and terminator of *YPT1* and expressed in a *ypt1Δ* background.

We previously showed that the *ypt1-1* chromosomal mutation confers severe selective and nonselective autophagy blocks (Segev and Botstein, 1987; Lipatova *et al.*, 2012). In contrast, the *ypt1-T40A* allele was suggested to confer an endosome-to-Golgi transport block (Sclafani *et al.*, 2010). First, we determined whether, like *ypt1-1*, the two mutations *ypt1-T40A* and *ypt1-T40K* expressed from a plasmid over the null confer an autophagy defect. Nonselective autophagy was determined by survival under nitrogen starvation; the selective autophagy cytosol-to-vacuole pathway (CVT) was determined by processing of Ape1. Like *ypt1-1*, both *ypt1-T40A* and *ypt1-T40K* alleles, when expressed from a plasmid over the null, confer a block in selective and nonselective autophagy (Figure 1, A and B). Second, we tested the interaction of Ypt1 and Atg11 using the yeast two-hybrid assay. We recently showed that, whereas the Ypt1 wild-type protein interacts with its autophagy-specific effector Atg11, the Ypt1-T40K mutant protein does not (Lipatova *et al.*, 2012). Like Ypt1-T40K, Ypt1-T40A is defective in the Ypt1-Atg11 interaction (Figure 1C). Therefore the *ypt1-T40A* mutation appears to confer the same autophagy defects as the *ypt1-T40K*.

To further characterize the autophagy-specific *ypt1* mutations, we tested their effect on the localization of membrane proteins. One such membrane protein is Snc1, a vesicle soluble *N*-ethylmaleimide–sensitive factor attachment protein receptor that recycles through endosomes for multiple rounds of function between the Golgi and the PM. Intracellular accumulation of GFP-tagged Snc1 has been used as a marker of an endosome-to-Golgi transport block (e.g., in *ypt31Δ/ypt32ts* mutant cells; Lewis *et al.*, 2000; Chen *et al.*, 2005) and was used as an indication for such a block in *ypt1-T40A* mutant cells (Sclafani *et al.*, 2010). We recently showed, however, that intracellular accumulation of green fluorescent protein (GFP)–tagged Snc1 also occurs as a result of an ER-to-Golgi block (e.g., in *ypt1-A136D* temperature-sensitive mutant cells; Zou *et al.*, 2012) and, as shown later, also as a result of a defect in ER-phagy.

First, we tested the effect of the *ypt1-1* mutation on the localization of Snc1-GFP. We determined the extent of colocalization of intracellular Snc1-GFP with an ER marker, Hmg1, and with endosomes (using a pulse and short chase with the membrane fluorescent dye FM4-64). Endogenous Hmg1 was tagged with mCherry in wild-type and *ypt1-1* and *ypt31Δ/ypt32ts* mutant cells (without expressing Snc1-GFP). Whereas in wild-type and *ypt31Δ/ypt32ts* mutant cells Hmg1-mCherry localizes to rings around nuclei (Huh *et al.*, 2003), the majority of *ypt1-1* mutant cells contain aberrant structures in addition to the rings (Figure 2A). This was true also for another ER protein, the translocon subunit Sec61, and a nuclear pore subunit, Nup60 (Figure 2, B and C; Huh *et al.*, 2003). In wild-type cells, Snc1-GFP localizes to the PM and to a few small puncta that colocalize with endosomes and not with the ER. In *ypt31Δ/ypt32ts* mutant cells, which are defective in endosome-to-Golgi transport (Chen *et al.*, 2005), there is intracellular accumulation of Snc1-GFP, which localizes to endosomes but not to the ER (Figure 3, A and B). We find that *ypt1-1* mutant cells also accumulate

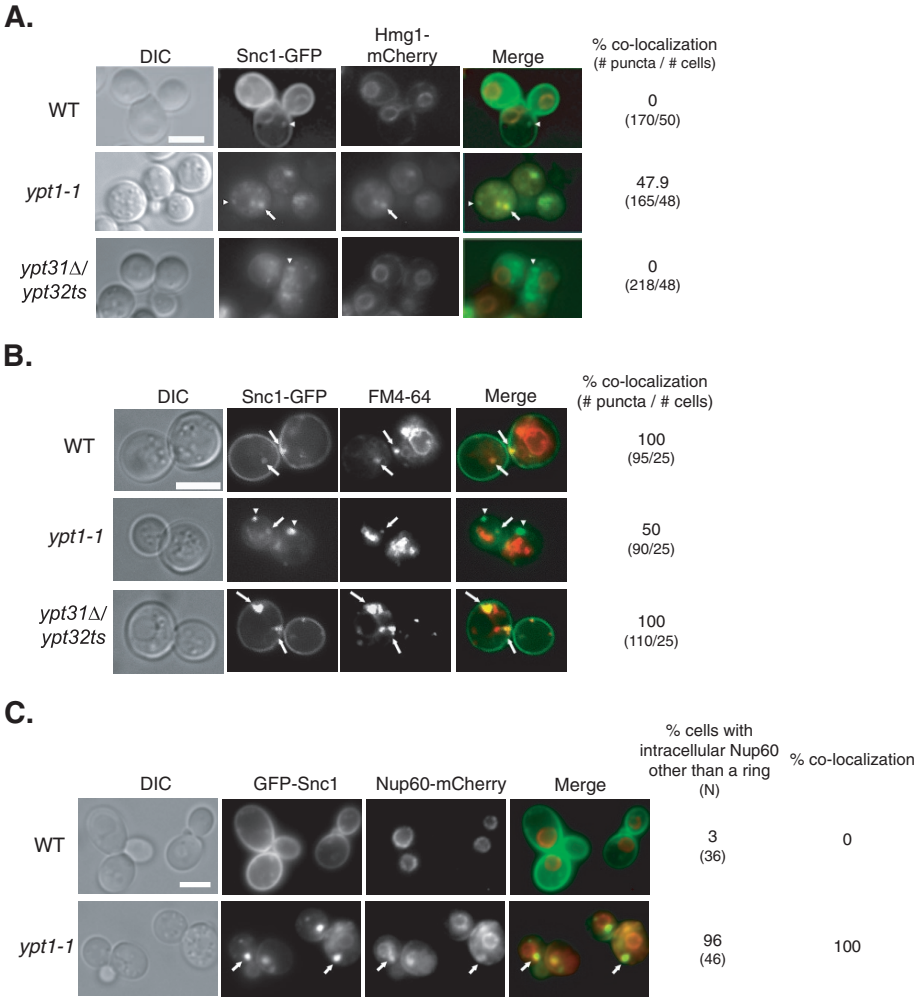

FIGURE 3: GFP-tagged Snc1 accumulates in the ER of *ypt1-1* mutant cells. (A) Colocalization of Snc1-GFP with the ER marker Hmg1 in *ypt1-1*, but not in wild-type or *ypt31Δ/32ts* mutant cells. Wild-type and *ypt1-1* and *ypt31Δ/32ts* mutant cells expressing Hmg1-mCherry from its endogenous locus and Snc1-GFP from a 2 μ plasmid were visualized by live-cell fluorescence microscopy. Left to right, DIC, GFP, mCherry, merge, percentage colocalization of Snc1-GFP puncta with Hmg1-mCherry (number of GFP puncta/number of cells visualized). Arrows point to GFP puncta that colocalize with mCherry; arrowheads point to GFP puncta that do not colocalize with mCherry. In wild-type and *ypt31Δ/32ts* mutant cells, Hmg1-mCherry localizes to rings around nuclei (Huh *et al*., 2003), which do not overlap with Snc1-GFP puncta. In contrast, in *ypt1-1* mutant cells, about half of the Snc1-GFP puncta colocalize with Hmg1. (B) Only half of the intracellular Snc1-GFP is in endosomes of *ypt1-1* mutant cells. Endosomes of cells expressing Snc1-GFP, as in Figure 1A, were labeled with FM4-64 and chased for 5 min. Cells were visualized by live-cell microscopy for GFP and FM4-64. Left to right, DIC, GFP, FM4-64, merge, and percentage colocalization of GFP with FM4-64 (number of GFP puncta/number of cells visualized). Arrows point to GFP puncta that colocalize with FM4-64; arrowheads point to GFP puncta that do not colocalize with FM4-64. Whereas all intracellular Snc1-GFP puncta overlap with endosomes in wild-type and *ypt31Δ/32ts* mutant cells, only half localize to endosomes *in ypt1-1* mutant cells. (C) The nuclear pore marker Nup60-mCherry colocalizes with intracellular GFP-Snc1. Wild-type and *ypt1-1* mutant cells expressing endogenously tagged Nup60-mCherry and GFP-Snc1 from a 2 μ plasmid were visualized by live-cell microscopy. Left to right, DIC, GFP, mCherry, merge, percentage of cells with intracellular aberrant Nup60-mCherry (*N*, number of cells visualized), and percentage colocalization (percentage of cells in which intracellular GFP-Snc1 colocalizes with Nup60-mCherry). Arrows point to GFP puncta that colocalize with mCherry. In wild-type cells, Nup60-mCherry localizes to rings around nuclei (Huh *et al*., 2003). Almost all *ypt1-1* mutant cells (96%) contain aberrant structures other than the rings in which Nup60-mCherry colocalizes with GFP-Snc1. Bars, 5 μm. Results represent at least two independent experiments.

intracellular Snc1-GFP as both small and very large puncta. Whereas ~50% of the intracellular Snc1-GFP puncta in *ypt1-1* mutant cells localize to endosomes (smaller puncta), ~50% colocalize with the ER marker (larger puncta; Figure 3, A and B). This result suggests that transport of Snc1-GFP from the ER of *ypt1-1* mutant cells is hindered but that some Snc1-GFP reaches the PM and can be recycled through endosomes.

Both Snc1 and Hmg1 are integral membrane proteins. To determine whether membrane-associated proteins also accumulate on membranes in *ypt1-1* mutant cells, we tagged endogenous Nup60 with mCherry in wild-type and mutant cells overexpressing GFP-Snc1. We verified that GFP-Snc1 (tagged at the N-terminus), like Snc1-GFP (used earlier), accumulates in the ER of *ypt1-1* mutant cells (Supplemental Figure S1). In wild-type cells expressing both tagged proteins, intracellular GFP-Snc1 does not colocalize with the Nup60-mCherry rings. In *ypt1-1* mutant cells, however, Nup60-mCherry accumulates in puncta in addition to the rings. The Nup60-mCherry puncta colocalize with Snc1-GFP (Figure 3C). Together these results show that *ypt1-1* mutant cells accumulate overexpressed membrane and membrane-associated proteins in aberrant ER structures.

Because a subset of Snc1 accumulations in *ypt1-1* mutant cells colocalize with endosomes, a phenomenon also observed in wild-type cells, we reasoned that these puncta arise through the normal process of Snc1 recycling from the PM to endosome. To establish that the larger accumulations in *ypt1-1* mutant cells, which do not colocalize with endosomes, are not due to a PM recycling defect, we used GFP-Snc1-PEM, a mutant that cannot be internalized once it reaches the PM (Lewis *et al*., 2000). Thus intracellular accumulation of GFP-Snc1-PEM would be a result of a block in its transport to the PM and not PM recycling. We previously showed that *ypt31Δ/32ts* mutant cells, which are defective in endosome-to-Golgi transport, do not accumulate intracellular GFP-Snc1-PEM (Chen *et al*., 2005). Accumulation of intracellular GFP-Snc1-PEM and its colocalization with two ER markers, Hmg1 and Sec61, was determined in wild-type and *ypt1-1* mutant cells. In wild-type cells, all the GFP-Snc1-PEM localizes to the PM and does not colocalize with Hmg1-mCherry or Sec61-mCherry rings. In *ypt1-1* mutant cells GFP-Snc1-PEM is found on

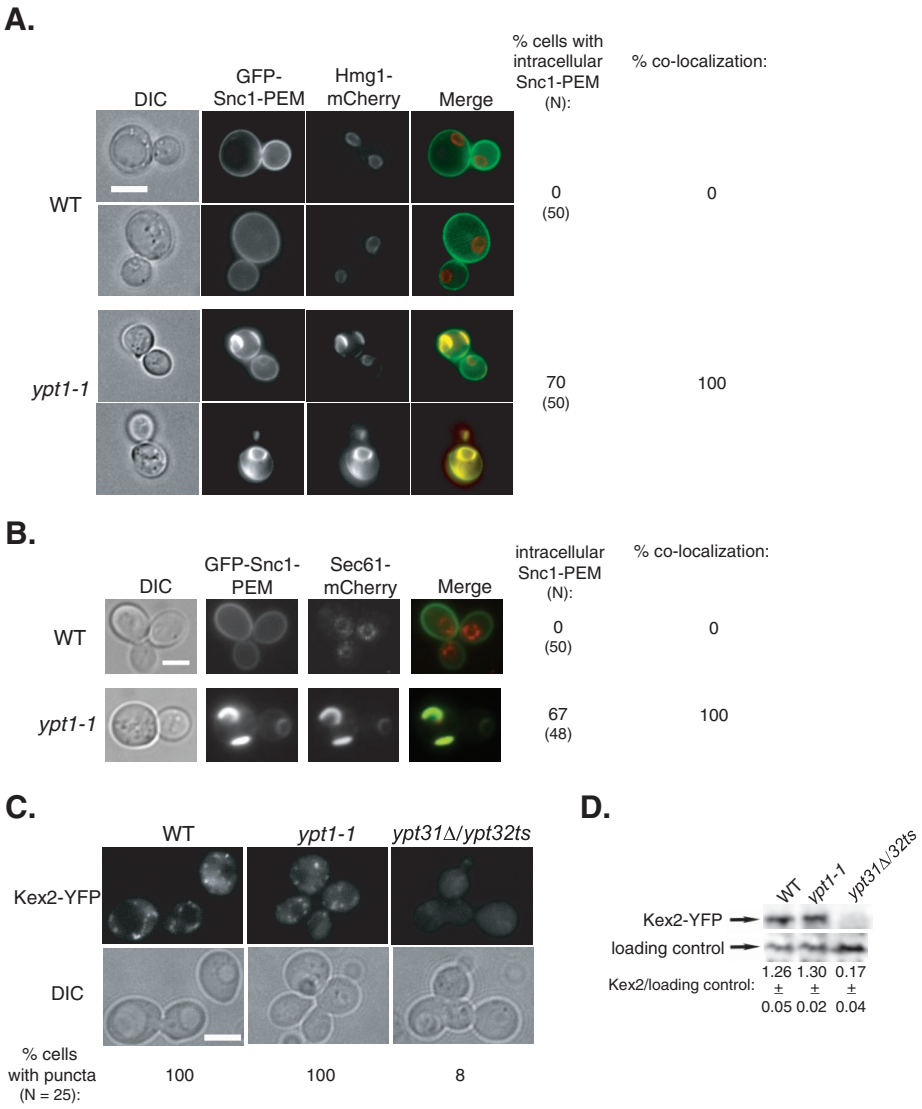

FIGURE 4: Accumulation of tagged proteins in *ypt1-1* mutant cells is not due to an endosome-to-Golgi recycling defect. (A, B) GFP-Snc1-PEM, which cannot be internalized, accumulates in the ER in *ypt1-1* mutant cells. Wild-type and *ypt1-1* mutant cells expressing Hmg1-mCherry (A) or Sec61-mCherry (B) from their endogenous loci and GFP-Snc1-PEM from a 2 μ plasmid were visualized by live-cell fluorescence microscopy. left to right: DIC, GFP, mCherry, merge, percentage of cells with intracellular GFP-Snc1-PEM (*N*, number of cells visualized), and percentage colocalization (percentage of cells in which intracellular GFP-Snc1-PEM colocalizes with Hmg1 or Sec61). In wild-type cells all the GFP-Snc1-PEM is on the PM and does not colocalize with the Hmg1 or Sec61 rings. In *ypt1-1* mutant cells, intracellular GFP-Snc1-PEM accumulates in ~70% of the cells and completely colocalizes with Hmg1 and Sec61. (C, D) Endosome-to-Golgi recycling is not defective in *ypt1-1* mutant cells. Endogenous Kex2-YFP was expressed in wild-type and *ypt1-1* and *ypt31Δ/32ts* mutant cells. Cells were visualized by live-cell fluorescence microscopy (C). Left to right, DIC, YFP, and percentage of cells with GFP puncta (*N*, number of cells visualized). Lysates from wild-type and *ypt1-1* and *ypt31Δ/32ts* mutant cells expressing Kex2-YFP were subjected to immunoblot analysis using anti-GFP antibodies (D). Bands were quantified, and the ratio of Kex2 over the loading control is shown; ±, SD. In wild-type and *ypt1-1* mutant cells, the level of Kex2-YFP is similar, and Kex2-YFP puncta were observed. In contrast, in *ypt31Δ/32ts* mutant cells, which are defective in endosome-to-Golgi transport, the level of Kex2-YFP is significantly lower, and almost no Kex2-YFP puncta were seen. Bar, 5 μm. Results represent at least two independent experiments.

the PM; however, ~70% of the mutant cells also demonstrate intracellular accumulation of GFP-Snc1-PEM. Of importance, this intracellular GFP-Snc1-PEM completely colocalizes with Hmg1-mCherry and Sec61-mCherry (Figure 4, A and B). These results indicate that in *ypt1-1* mutant cells GFP-Snc1-PEM transport is blocked at the ER before it reaches the PM. Moreover, intracellular accumulation of Snc1-PEM incapable of being internalized in *ypt1-1* mutant cells indicates that the defect causing abnormal accumulation is not in the endosome-to-Golgi transport step.

To further verify that *ypt1-1* mutant cells are not defective in endosome-to-Golgi transport, we examined a second cargo, Kex2, which cycles between the *trans*-Golgi and endosomes. In cells defective in endosome-to-Golgi transport, Kex2 is shuttled to the vacuole for degradation. We previously used Kex2-YFP to establish the endosome-to-Golgi transport defect of *ypt31Δ/32ts* mutant cells (Chen *et al.*, 2005). In *ypt31Δ/32ts* mutant cells Kex2-YFP does not show the typical Golgi puncta and is degraded in the vacuole. In contrast, in wild-type and *ypt1-1* mutant cells, Kex2-YFP localizes to puncta and is stable (Figure 4, C and D). Together the Snc1-PEM and Kex2 results support the idea that *ypt1-1* mutant cells are not defective in endosome-to-Golgi transport. Therefore the intracellular accumulation of GFP-tagged Snc1 in *ypt1-1* is not due to a PM recycling defect but instead is due to a transport block at the ER.

Next we determined whether, like *ypt1-1*, *ypt1-T40A* and *ypt1-T40K* expressed from a plasmid over the null confer accumulation of GFP-tagged Snc1 in the ER. Whereas all intracellular Snc1-GFP localizes to endosomes in wild-type cells, only ~50% does so in *ypt1-1* (Figure 3B), *ypt1-T40K*, and *ypt1-T40A* mutant cells (Figure 5A). In addition, whereas all the GFP-Snc1-PEM protein localizes to the PM of wild-type cells, ~70% of the *ypt1-1*, *ypt1-T40K*, and *ypt1-T40A* mutant cells accumulate intracellular GFP-Snc1-PEM, which completely colocalizes with the ER marker Hmg1 (Figures 4A and 5B). Finally, like *ypt1-1* (Figure 4, C and D), neither *ypt1-T40K* nor *ypt1-T40A* mutant cells are defective in recycling of Kex2-YFP (Figure 5, C and D). These results show that the two *YPT1* mutant alleles *ypt1-T40A* and *ypt1-T40K*, which are defective in autophagy and not in the exocytic pathway, accumulate overexpressed GFP-tagged Snc1 in the ER. Moreover, this accumulation is not due to an endosome-to-Golgi transport defect.

The accumulation of large puncta of fluorescently tagged Snc1 with Hmg1, Sec61, and Nup60 in *ypt1-1* mutant cells suggests that these membrane or membrane-associated proteins accumulate on aberrant ER structures. To support this idea, we used immuno–electron microscopy (EM) of wild-type and *ypt1-1* mutant cells expressing Snc1-GFP. Anti-Hmg1 antibodies were used to mark the ER (Hmg1 was not tagged). The elongated

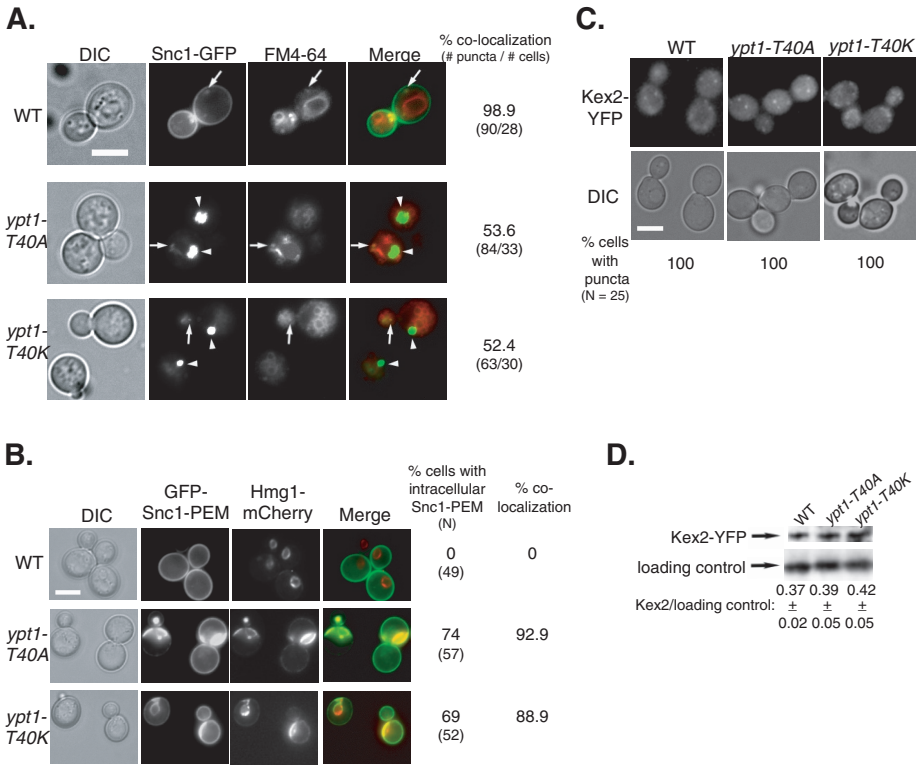

FIGURE 5: The *YPT1-T40A* mutation, like *YPT1-T40K*, confers Snc1-GFP accumulation in the ER but not endosome-to-Golgi transport defects. The three strains used here are *YPT1* (WT), *ypt1-T40K*, and *ypt1-T40A* allele (as in Figure 1). (A) Half of the intracellular Snc1-GFP localizes to endosomes in *ypt1-T40A* and *ypt1-T40K* mutant cells. The endosomes of cells expressing Snc1-GFP were labeled with FM4-64, and cells were visualized using live-cell microscopy (as in Figure 3B). Left to right, DIC, GFP, FM4-64, merge, percentage colocalization of Snc1-GFP with endosomes (number of GFP puncta/number of cells visualized). Arrows point to GFP puncta that colocalize with FM4-64; arrowheads point to GFP puncta that do not colocalize with FM4-64. About 50% of the intracellular Snc1-GFP colocalizes with FM4-64 in *ypt1-T40A* and *ypt1-T40K*, as compared with ~100% colocalization in wild-type cells. (B) Intracellular GFP-Snc1-PEM localizes to the ER in both *ypt1-T40K* and *ypt1-T40A* mutant cells. Cells expressing GFP-Snc1-PEM and the endogenously tagged ER marker Hmg1-mCherry (as in Figure 3A) were visualized by live-cell fluorescence microscopy. Left to right, DIC, GFP, mCherry, merge, percentage of cells with intracellular GFP-Snc1-PEM (*N*, number of cells visualized), and percentage colocalization (percentage of cells in which intracellular GFP-Snc1-PEM colocalizes with Hmg1). In wild-type cells all the GFP-Snc1-PEM is on the PM and does not colocalize with Hmg1 rings. In *ypt1-T40A* and *Ypt1-T40K* mutant cells, ~90% of the intracellular GFP-Snc1-PEM colocalizes with Hmg1. (C) Kex2 recycling is not defective in *ypt1-T40K* and *ypt1-T40A* mutant cells. Endogenous Kex2-YFP was expressed in wild-type and *ypt1-T40K* and *ypt1-T40A* mutant cells. Top, cells were visualized by live-cell fluorescence microscopy (as in Figure 4C). Left to right, DIC, YFP, and percentage of cells with intracellular GFP puncta (*N*, number of cells visualized). (D) Immunoblot analysis of Kex2-YFP. Lysates from wild-type and *ypt1-T40K* and *ypt1-T40A* mutant cells expressing Kex2-YFP were subjected to immunoblot analysis using anti-GFP antibodies (as in Figure 4D). Bands were quantified and the ratio of Kex2 over the loading control is shown; ±, SD. Like wild-type cells, both *ypt1-T40K* and *ypt1-T40A* mutant cells show Kex2-YFP puncta and similar level of Kex2-YFP. Bar, 5 μm (A–C). Results represent at least two independent experiments.

membrane structures identified as ER in wild-type cells are Hmg1 positive, and their morphology is consistent with ER membranes identified with other protein markers in earlier immuno-EM studies using similar methods (Preuss *et al.*, 1991). In *ypt1-1* mutant cells, there is an accumulation of aberrant structures that appear tubular-vesicular in nature and form aggregates. Unlike lipid droplets, these structures are membrane bound and contain electron-dense material. Of interest, these structures are decorated with anti-Hmg1 antibodies, indicative of their ER origin. We observed an >20-fold increase in membrane-associated Hmg1 in *ypt1-1* compared with wild-type cells (Figure 6 and Supplemental Table S1). These Hmg1-positive aggregates of aberrant membranes mostly likely represent the fluorescent Hmg1-mCherry puncta observed in the fluorescence microscopy experiments in *ypt1-1* mutant cells. Together these results indicate that *ypt1-1* mutant cells accumulate overexpressed fluorescently tagged proteins on aberrant ER structures.

A role for Ypt1 in ER-phagy

We hypothesized that in wild-type cells, excess and misfolded membrane proteins are shuttled from the ER for degradation in the vacuole (the yeast lysosome) through the autophagy pathway. In contrast, because *ypt1-1* mutant cells are defective in autophagy, they accumulate aberrant ER structures filled with excess proteins, which have stalled before reaching the vacuole. Moreover, such accumulation should induce the UPR in the ER.

To test the first part of this idea, we analyzed the intracellular accumulation of the nonrecyclable GFP-Snc1-PEM protein in *pep4Δ* mutant cells, which are compromised for protein degradation in the vacuole (Jones *et al.*, 1982). Because GFP-Snc1-PEM cannot get to the vacuole through endosomes, its accumulation in the vacuole in *pep4Δ* mutant cells is due to shuttling from the exocytic pathway. Whereas no intracellular GFP-Snc1-PEM accumulates in wild-type cells (Figure 4A), ~80% of the *pep4Δ* mutant cells accumulate intracellular GFP-Snc1-PEM. Moreover, this internal GFP-Snc1-PEM accumulates inside the vacuole (labeled by FM4-64) and does not colocalize with the ER marker Hmg1 (Figure 7, A and B). In contrast, deletion of *PEP4* in *ypt1-1* mutant cells does not affect the localization of GFP-Snc1-PEM, which accumulates in the ER of ~70% of the cells and not in the vacuole (compare Figures 4A and 7, A and B). To further support this microscopy observation, the level of GFP-Snc1-PEM in the four yeast strains was determined using an immunoblot analysis. In wild-type cells (*YPT1*), deletion of *PEP4* results in accumulation of GFP-Snc1-PEM. In contrast, in *ypt1-1* mutant cells, the level of GFP-Snc1-PEM is higher than in wild-type cells and is similar in *PEP4* and *pep4Δ* cells (Figure 7C). These results support the idea that in wild-type cells, excess GFP-Snc1-PEM is shuttled to the vacuole for degradation, and this transport is defective in *ypt1-1* mutant cells.

Overexpression and accumulation of fluorescently tagged ER proteins might generate a greater population of misfolded proteins. We reasoned that the UPR would be induced in cells that accumulate such proteins. To test this idea, we determined the degree of UPR induction in wild-type and *ypt1-1* mutant cells expressing

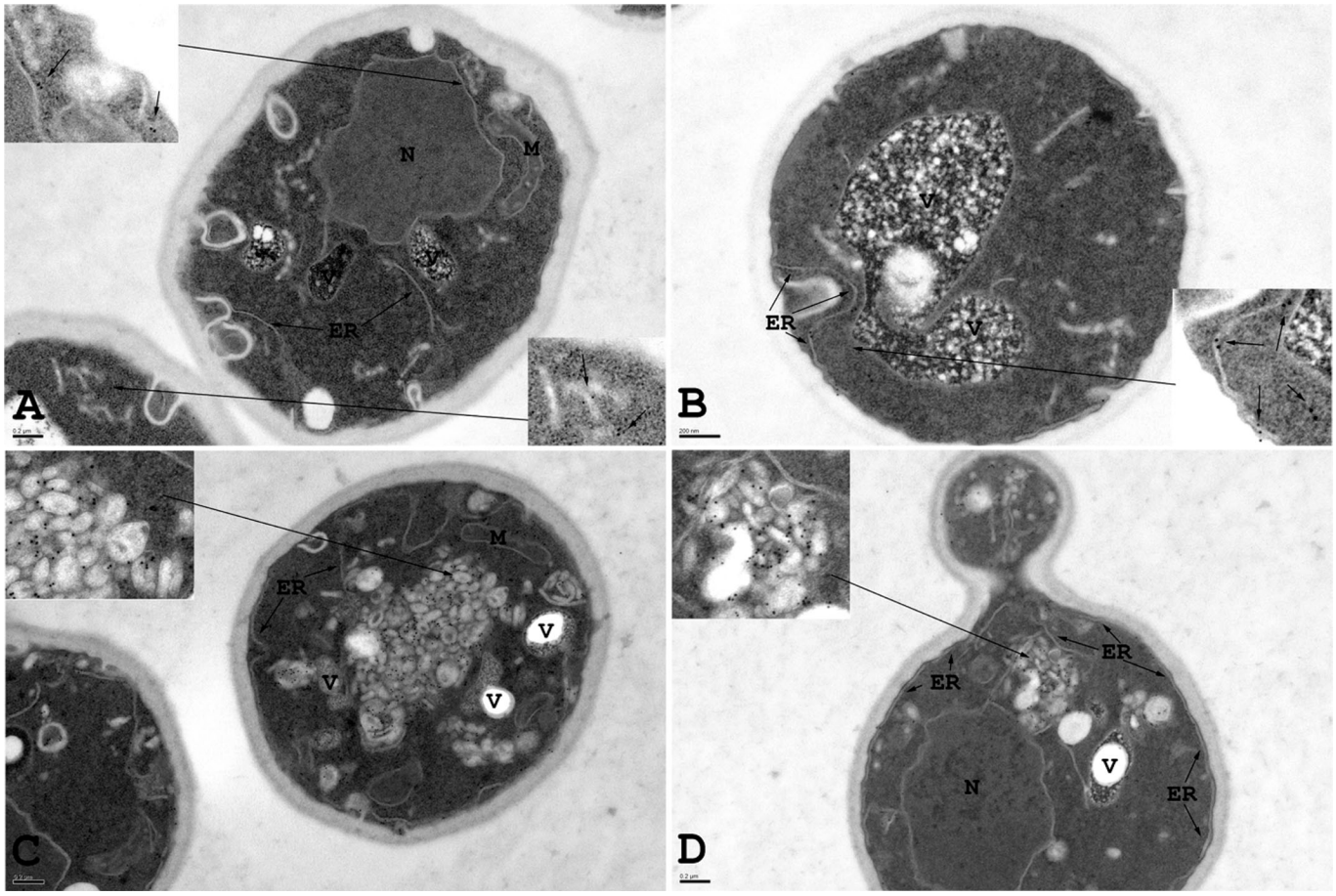

FIGURE 6: Aberrant ER accumulation in *ypt1-1* mutant cells overexpressing Snc1-GFP. Immuno-EM analysis was done with wild-type and *ypt1-1* mutant cells expressing Snc1-GFP. Wild-type and *ypt1-1* mutant cells expressing Snc1-GFP were grown to log phase, fixed, and processed for immuno-EM using anti-Hmg1 antibodies. Insets show enlarged view of ER structures labeled with gold particles. (A, B) In wild-type cells, Hmg1, an ER marker, is present exclusively on elongated ER membranes. (C, D) In *ypt1-1* mutant cells Hmg1 is present on aberrant membrane structures. ER, endoplasmic reticulum; M, mitochondria; N, nucleus; V, vacuole. Bar, 200 nm. Results represent two independent experiments; quantification is shown in Supplemental Table S1.

Snc1-GFP. Cells were transformed with a second plasmid encoding the lacZ gene behind four repeats of a UPR element, and the level of β-galactosidase (βgal) in cell lysates was determined (Kruse *et al.*, 2006). UPR induction was 10-fold greater in *ypt1-1* mutant cells than in wild-type cells. In contrast, no such induction was observed in *ypt31Δ/32ts* mutant cells under conditions in which they accumulate intracellular Snc1-GFP (Figure 8, A and B). Furthermore, UPR is induced in both *ypt1-T40K* and *ypt1-T40A* mutant cells overexpressing Snc1-GFP (Figure 8C). These results suggest that *ypt1-1*, *ypt1-T40K*, and *ypt1-T40A*, but not *ypt31Δ/32ts*, mutant cells accumulate misfolded Snc1-GFP in their ER. Therefore these *ypt1* mutant cells, which are not defective in ER-to-Golgi transport, are defective in ER-phagy.

To verify that the ER-phagy pathway is independent of the Golgi, we determined the effect of Snc1-GFP overexpression on UPR in *sec7-4* mutant cells. Sec7 is a GEF for Arf GTPases, which functions in the Golgi (Franzusoff *et al.*, 1991). The *sec7-4* mutation is in the GEF domain of Sec7 (Jones *et al.*, 1999). Snc1-GFP accumulates in *sec7-4* mutant cells, especially at 37°C (Figure 8D). Even though the UPR response can be induced by tunicamycin, however, it is not induced in sec7-4 mutant cells overexpressing Snc1-GFP (Figure 8, E and F).

A role for the Trs85-Ypt1-Atg11 module in ER-phagy

If Ypt1 regulates shuttling of excess GFP-tagged Snc1 through the autophagic pathway to the vacuole for degradation, we expect that it does so in the context of the autophagy-specific module, including the specific GEF and effector. Recently we showed that the GEF/Trs85-Ypt1-effector/Atg11 module regulates the onset of selective autophagy (Lipatova *et al.*, 2012). We therefore tested the role of the Trs85-Ypt1-Atg11 module in ER-phagy.

GEF mutations are expected to result in phenotypes similar to those of mutations in their Ypt substrates. We proposed that Trs85-containing TRAPPIII and Trs130-containing TRAPPII function as GEFs for Ypt1 and Ypt31, respectively (Morozova *et al.*, 2006; Zou *et al.*, 2012). Both *trs85Δ* and *trs130ts* mutant cells accumulate intracellular Snc1-GFP (Zou *et al.*, 2012). The effect of overexpression of Snc1-GFP in *trs85Δ* and *trs130ts* mutations on UPR was determined. Similar to *ypt1-1* mutant cells, UPR is induced in *trs85Δ* mutant cells expressing Snc1-GFP. In contrast, similar to *ypt31Δ/32ts* mutant cells, UPR is not induced in *trs130ts* mutant cells under conditions in which they accumulate intracellular Snc1-GFP (Figure 8, A and B). These results show that the nature of Snc1-GFP accumulation in *ypt1-1* and *trs85Δ* mutant cells is distinct from its accumulation in *ypt31Δ/32ts* and *trs130ts*, which are

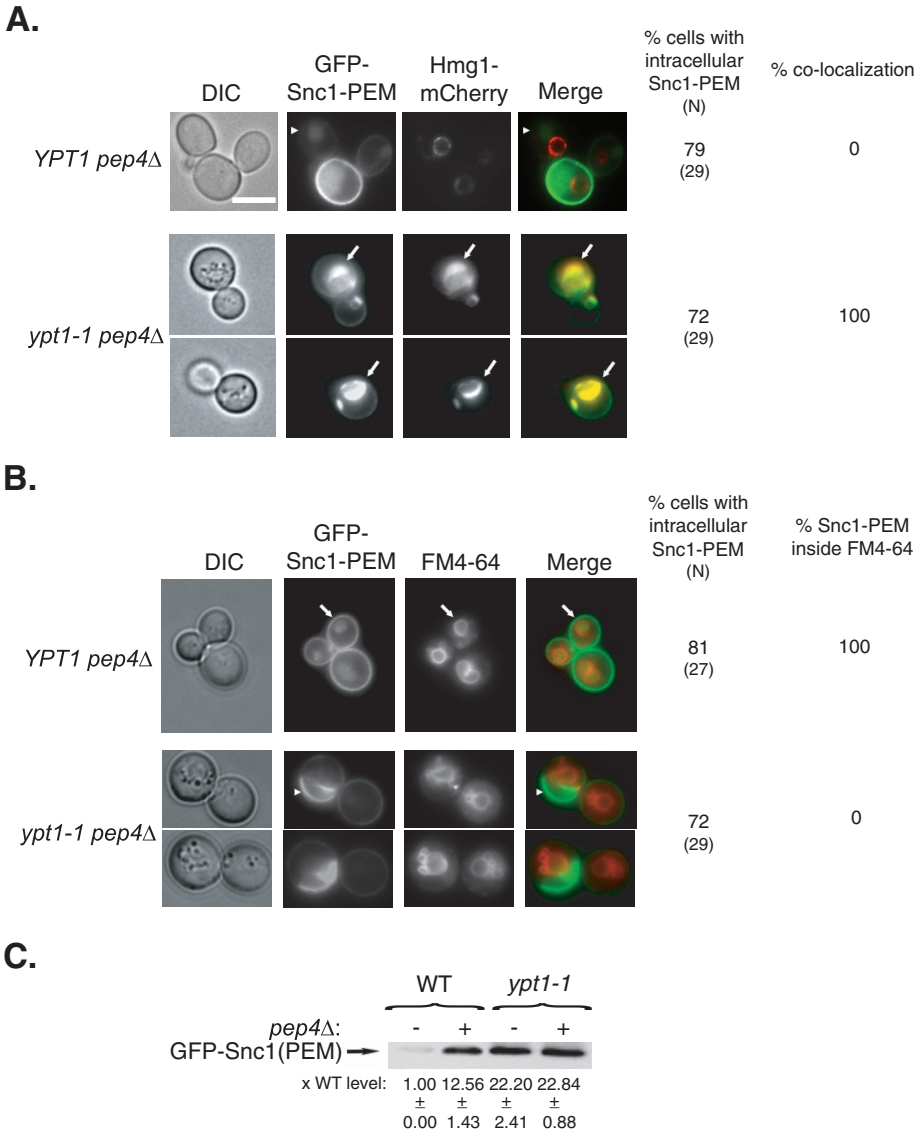

FIGURE 7: GFP-Snc1-PEM accumulates in the vacuole of *pep4Δ*, but not *ypt1-1 pep4Δ*, mutant cells. (A) Accumulation of intracellular GFP-Snc1-PEM outside the ER of *YPT1* (WT) *pep4Δ* cells defective in vacuolar degradation. GFP-Snc1-PEM was expressed from a 2 μ plasmid and mCherry-Hmg1 from its endogenous locus (as in Figure 4A) in *YPT1* pep4Δ and *ypt1-1 pep4Δ* mutant cells. Cells were visualized by live-cell fluorescence microscopy. Left to right, DIC, GFP, mCherry, merge, percentage of cells with intracellular GFP-Snc1-PEM (*N*, number of cells visualized), and percentage colocalization (percentage of cells in which intracellular GFP-Snc1-PEM colocalizes with Hmg1-mCherry). In *YPT1* (WT) *pep4Δ* cells, intracellular GFP-Snc1-PEM does not colocalize with the Hmg1 rings (arrowheads). In *ypt1-1 pep4Δ* double mutant cells, intracellular GFP-Snc1-PEM colocalizes with Hmg1 (arrows). (B) Intracellular GFP-Snc1-PEM accumulates inside the vacuole of *YPT1 pep4Δ* but not *ypt1-1 pep4Δ* mutant cells. The vacuolar membrane of *YPT1 pep4Δ* and *ypt1-1 pep4Δ* mutant cells expressing GFP-Snc1-PEM was labeled with FM4-64. Cells were visualized by live-cell microscopy. Left to right, DIC, GFP, FM4-64, merge, percentage of cells with intracellular GFP-Snc1-PEM (*N*, number of cells visualized), and percentage localization of intracellular GFP-Snc1-PEM inside the vacuole. Arrows point to GFP localized inside FM4-64-labled vacuoles *YPT1* (WT) *pep4Δ* cells; arrowheads point to GFP that does not localize inside FM4-64-labled vacuoles in *ypt1-1 pep4Δ* double mutant cells. (C) Accumulation of GFP-Snc1-PEM in *ypt1-1* mutant cells is not dependent on the vacuolar Pep4 protease. The protein level of GFP-Snc1-PEM in lysates of wild-type and *ypt1-1* mutant cells with or without *pep4Δ* was determined using immunoblot analysis and anti-GFP antibodies. Bands were quantified, and the ratio of GFP-Snc1-PEM in mutant versus wild-type cells is shown at the bottom; ±, SD. The level of GFP-Snc1-PEM is higher in *pep4Δ* mutant cells than in wild-type cells, indicating that the protein is degraded in the vacuole. In contrast, the high level of GFP-Snc1-PEM In *ypt1-1* mutant cells is not dependent on *pep4Δ*, indicating that the protein does not reach the vacuole. Bar, 5 μm. Results represent at least two independent experiments.

defective in endosome-to-Golgi transport (Chen *et al.*, 2005; Zou *et al.*, 2012). Moreover, because both *ypt1-1* and *trs85Δ* are defective in autophagy, these results suggest that accumulation of excess proteins in the ER of these mutant cells is due to a block in the autophagic pathway.

We showed that overexpression of Ypt1 can suppress the CVT phenotype of *trs85Δ* mutant cells (Lipatova *et al.*, 2012). We tested whether it can also suppress the ER-phagy phenotypes of *trs85Δ* mutant cells. Overexpression of Ypt1 but not Ypt1-T40K mutant protein can suppress both the intracellular accumulation of Snc1-GFP and UPR induction in *trs85Δ* mutant cells (Figure 9, A and B, respectively). These results suggest that Trs85 functions upstream of Ypt1 in clearing out excess ER proteins through autophagy.

We also previously showed that Atg11 acts as an autophagy-specific Ypt1 effector, and an Atg11-Ypt1-T40K fusion protein can suppress the autophagy defects of *ypt1-1* mutant cells (Lipatova *et al.*, 2012). Here we tested whether this is also true for the ER accumulation of GFP-Snc1 and UPR induction. First, intracellular accumulation of GFP-Snc1-PEM is observed in *atg11Δ* mutant cells, and UPR is induced in these cells (Figure 10, A and B), implicating Atg11 in ER-phagy. Second, the Atg11-Ypt1-T40K fusion protein can rescue both the GFP-Snc1-PEM intracellular accumulation and UPR induction of *ypt1-1* mutant cells. In contrast, neither the Ypt1-T40K mutant protein (which cannot interact with Atg11) nor Atg11 alone can rescue the GFP-Snc1-PEM intracellular accumulation and UPR induction phenotypes of *ypt1-1* mutant cells (Figure 10, C and D). Together these results support the role of the Trs85-Ypt1-Atg11 module in shuttling excess ER proteins to the autophagy pathway for degradation.

DISCUSSION

On the basis of results presented here, we conclude that a Ypt/Rab GTPase module, consisting of the Trs85-containing TRAPPIII GEF, Ypt1, and the Atg11 effector, functions in ER-phagy. We recently showed that this module regulates the onset of selective autophagy (Lipatova *et al.*, 2012). However, the cellular compartment from

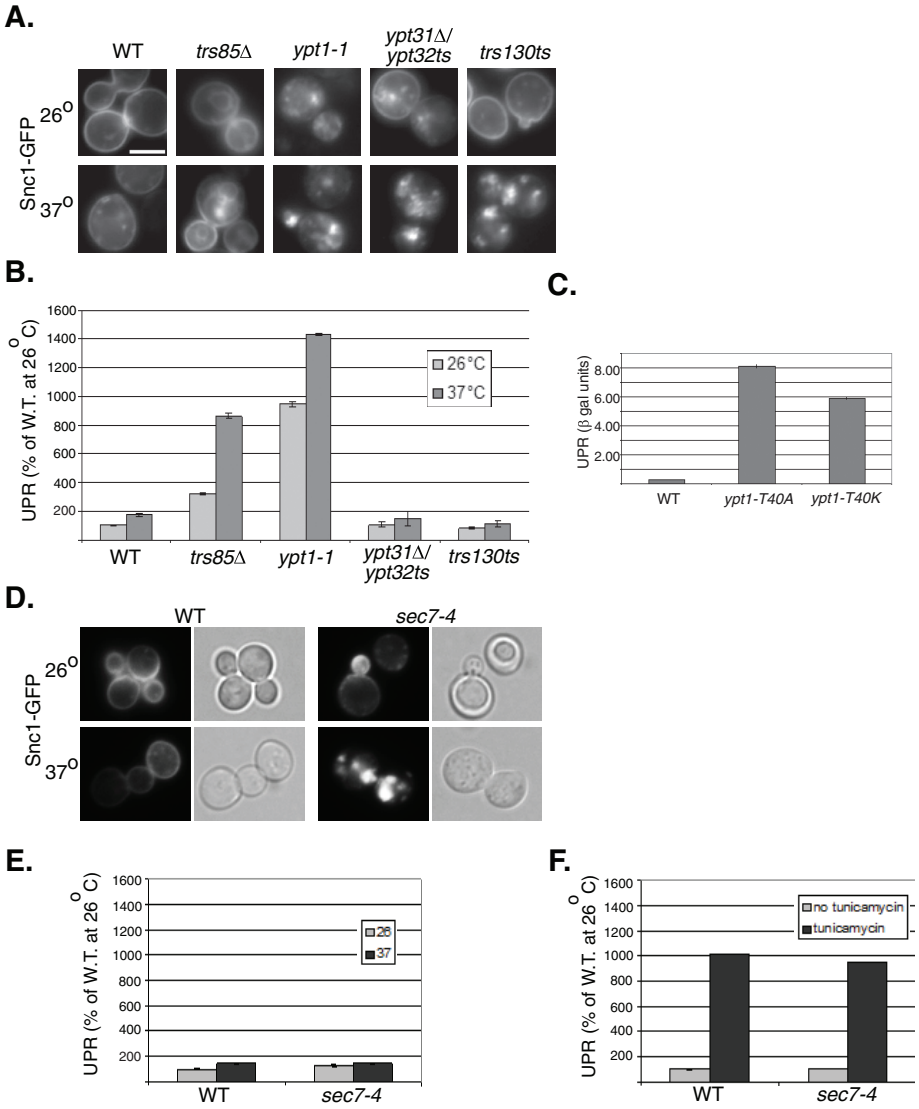

FIGURE 8: UPR is induced in *ypt1* and *trs85Δ* but not *ypt31Δ/32ts*, *trs130ts*, and *sec7-4* mutant cells expressing Snc1-GFP. (A) Snc1-GFP accumulates in internal puncta in *ypt1-1*, *trs85Δ*, *ypt31Δ/32ts*, and *trs130ts* mutant cells. Cells expressing Snc1-GFP from a 2 μ plasmid were grown at 26°C (top), shifted to 37°C for 90 min (bottom), and visualized by live-cell microscopy. Representative cells are shown (a minimum of 24 cells were visualized for each panel). All mutant cells accumulate internal Snc1-GFP at 37°C and to a lesser degree at 26°C. (B) UPR is induced in *ypt1-1* and *trs85Δ* but not *ypt31Δ/32ts* and *trs130ts* mutant cells. Cells expressing Snc1-GFP (as in A) were transformed with a second plasmid carrying the LacZ gene under a UPR-inducible promoter (Kruse *et al.*, 2006). Cells were grown at 26°C (light bars) and shifted to 37°C for 90 min (dark bars), and the induction of the UPR response was determined using the βGAL assay. UPR is expressed as percentage of the response of wild type at 26°C. The UPR response in *trs85Δ* and *ypt1-1* mutant cells is induced at 26°C and is even higher at 37°C. No such induction is observed in *ypt31Δ/32ts* or *trs130ts* mutant cells even under conditions in which these cells accumulate intracellular Snc1-GFP. (C) UPR is induced in *ypt1-T40K* and *ypt1-T40A* mutant cells expressing Snc1-GFP. UPR was determined in wild type and *ypt1* mutant cells expressing LacZ under a UPR-inducible promoter and Snc1-GFP (as in B). (D) Intracellular Snc1-GFP accumulates in *sec7-4* mutant cells. The experiment was done as described in A (50 cells were visualized for each panel). *sec7-4* mutant cells accumulate internal Snc1-GFP at 37°C and to a much lesser degree at 26°C. (E) UPR is not induced in *sec7-4* mutant cells. The experiment was done as described in B. No UPR induction is observed in *sec7-4* mutant cells even under conditions in which these cells accumulate intracellular Snc1-GFP. (F) UPR can be induced in wild-type and *sec7-4* mutant cells by tunicamycin. Cells were grown without tunicamycin (light bars) or with 5 μg/ml tunicamycin for 90 min (dark bars), and the induction of the UPR response was determined using the βGAL assay. Bar, 5 μm; error bars, SD (B, C, E, F). Results represent at least two independent experiments.

which membrane and cargo destined to autophagy originate was not known. We now show that the Trs85-Ypt1-Atg11 module regulates shuttling of tagged, overexpressed, and likely misfolded proteins from the ER to the autophagic pathway (Figure 10E). Two observations point to ER as the origin of the Ypt1-mediated autophagic branch: colocalization of the accumulated proteins with ER markers and induction of UPR in *trs85*, *ypt1*, and *atg11* mutant cells overexpressing tagged membrane proteins. Regulation of ER-phagy is distinctive from the role of Ypt1 in ER-to-Golgi transport because the *ypt1* mutants used here are not defective in ER-to-Golgi transport (Jedd *et al.*, 1995; Sclafani *et al.*, 2010). The *trs85Δ* and *atg11Δ* mutants are defective specifically in autophagy as well (Kim *et al.*, 2001; Meiling-Wesse *et al.*, 2005; Nazarko *et al.*, 2005).

In addition, results presented here argue against a role for Ypt1 in endosome-to-Golgi transport. Although our cumulative evidence points to a role for Ypt1 in ER-to-Golgi transport (Segev *et al.*, 1988; Segev, 1991; Jedd *et al.*, 1995) and ER-phagy (the present results), Sclafani *et al.* (2010) suggested that Ypt1 also plays a role in endosome-to-Golgi transport. This inference was based on the isolation of *ypt1* mutants that do not exhibit secretory defects but accumulate intracellular GFP-Snc1. This accumulation was taken as an indication for an endosome-to-*trans*-Golgi transport defect. Using one mutant isolated and characterized in the Sclafani study, *ypt1-T40A*, we show that the block in this mutant is not in endosome-to-Golgi transport but in ER-phagy. Therefore we conclude that Ypt1 does not regulate endosome-to-Golgi transport. We previously showed that that role is performed by the Ypt31/Ypt32 GTPases (Chen *et al.*, 2005).

On the basis of the present study, we propose a new paradigm for how Ypt/Rab GTPases coordinate intracellular trafficking pathways. In this paradigm, a single Ypt/Rab GTPase can regulate independent transport processes from the same compartment to more than one destination. We show here that in addition to the established role of Ypt1 in the regulation of transport of ER vesicles to the *cis*-Golgi, this GTPase also regulates transport of ER membranes—loaded with excess proteins—to autophagy. The separation of these two functions of Ypt1 was possible by the use of mutations that affect only autophagy and not ER-to-Golgi transport.

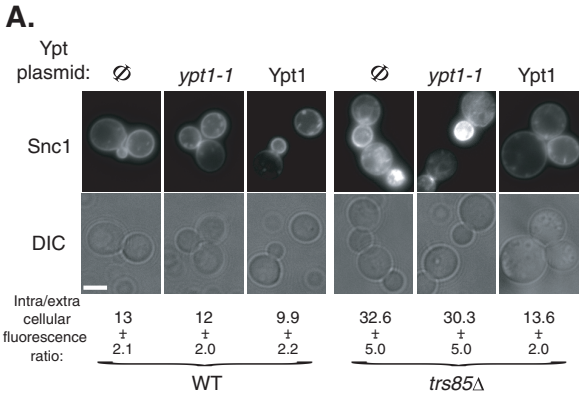

FIGURE 9: A role for the Trs85-Ypt1 interaction in ER-phagy. (A) Overexpression of Ypt1 suppresses the Snc1-GFP accumulation defect of *trs85Δ* mutant cells. Top, wild-type (left) and *trs85Δ* mutant cells (right) expressing Snc1-GFP from a 2 μ plasmid were transformed with a second plasmid expressing Ypt1-T40K (mutant) or Ypt1 (wild-type) proteins (Φ, empty vector control). Cells were visualized by live-cell microscopy; representative cells are shown: GFP (top) and DIC (bottom). Bar, 5 μm. Bottom, quantification of intracellular/extracellular fluorescence ratio. The ratio of fluorescence inside and outside cells was determined using ImageJ (40 cells for each strain). The level of intracellular fluorescence in *trs85Δ* mutant cells is three times higher than in wild-type cells, and this increase is suppressed if Ypt1 but not Ypt1-T40K mutant protein is overexpressed. (B) Overexpression of Ypt1 suppresses UPR induction in *trs85Δ* mutant cells. Cells were transformed with three plasmids expressing LacZ under a UPR promoter, Snc1-GFP, and Ypt1 (Φ, Ypt1, or Ypt1-T40K). Induction of the UPR was determined in cell lysates using the βGAL assay (as in Figure 8B). UPR is induced in *trs85Δ* mutant cells (Φ) when compared with wild type, and this induction is partially suppressed by overexpression of Ypt1 but not Ypt1-T40K protein. Results represent at least two independent experiments; error bars, SD.

The mechanism that allows Ypt1 to do that is to function in separate modules that contain process-specific GEF and effectors. The two proposed process-specific Ypt1 modules are TRAPPI and Uso1 in ER-to-Golgi transport, and TRAPPIII and Atg11 in ER-phagy (Figure 10E). An intriguing question is the nature of the cues that allow recruitment of the right Ypt/Rab module to the right membrane domain.

On the basis of the conservation of Ypt/Rabs, their GEF and effectors, and the autophagic machinery, we propose that Ypt1-dependent ER-phagy is also conserved. The importance of intracellular trafficking and autophagy in human disease (Howell *et al.*, 2006; Choi *et al.*, 2013) and the role that Ypt/Rabs play in autophagy (Chua *et al.*, 2011) have been recognized. Because Ypt/Rabs play essential roles in multiple processes, it is crucial to elucidate mechanisms that allow these regulators to function in trafficking intersections toward the goal of developing drugs that target a specific process without affecting the others.

MATERIALS AND METHODS

Strains, plasmids, and reagents

Strains and plasmids used in this study are summarized in Supplemental Tables S2 and S3, respectively. All chemical reagents were purchased from Fisher Scientific (Bridgewater, NJ), unless otherwise noted. Media components other than amino acids were purchased from US Biological (Swampscott, MA). ProtoGel for Western blots was purchased from National Diagnostics (Atlanta, GA). Amino acids, 2-nitrophenyl β-D-galactopyranoside, tunicamycin, and protease inhibitors were purchased from Sigma-Aldrich (St. Louis, MO). Glass beads were purchased from BioSpec Products (Bartlesville, OK). Restriction enzymes and buffers were purchased from New England BioLabs (Ipswich, MA). Dithiothreitol (DTT) was purchased from Invitrogen (Carlsbad, CA). FM4-64 was purchased from Molecular Probes (Eugene, OR). Antibodies used in this study include rabbit anti–GAL4-BD, mouse monoclonal anti-GFP (Santa Cruz Biotechnology, Santa Cruz, CA), mouse monoclonal anti-hemagglutinin (Covance, Madison, WI), goat anti-rabbit horseradish peroxidase (HRP) and goat anti-mouse-HRP (GE Healthcare UK, Chalfont St. Giles, United Kingdom), affinity-purified rabbit anti-Hmg1 (a gift from R. Wright, University of Minnesota), and anti-Ape1 (a gift from D. Klionsky, University of Michigan).

Plasmid and strain construction

Plasmids. pRS317-*ypt1-T40A* was made by site-directed mutagenesis of pRS317-*YPT1*. pRS327-*YPT1* and pRS327-*ypt1-T40K* were made by subcloning the *Bam*HI–*Cla*I fragments from pRS317-*YPT1* and pRS317-*ypt1-T40K*, respectively, into pRS327. pRS425-GFP-*SNC1* and pRS425-GFP-*SNC1* PEM were made by subcloning the *Bam*HI—*Psp*XI fragments from pRS406 GS and pRS406 GSSOM (Lewis *et al.*, 2000), respectively, into pRS425.

Yeast strains. Kex2 was tagged on the chromosome at the COOH terminus with yellow fluorescent protein (YFP) using PCR product from the Kex2-YFP from the Yeast Resource Center (University of Washington, Seattle, WA) and homologous recombination. Hmg1, Sec61, and Nup60 were tagged on the COOH termini according to the standard technique (Wach *et al.*, 1997).

Yeast culture conditions

Media preparation and yeast culture growth for all experiments were done as described (Segev and Botstein, 1987). For yeast two-hybrid assays, yeast cultures were grown overnight at 26°C in minimal (SD) media, normalized to the same density by OD_{600}, and spotted onto agar plates in serial dilutions. Plates for yeast two-hybrid assay, indicated in figure legends, were incubated at 26°C.

Protein expression analyses

To determine the level of Kex2-YPF and Ape1 proteins, lysates of exponentially growing or starved cells were prepared as described (Cheong and Klionsky, 2008) and subjected to immunoblot analysis using anti-GFP and anti-Ape1 antibodies, respectively. The expression level of yeast two-hybrid constructs was determined as previously described (Lipatova *et al.*, 2012). The level of GFP-Snc1-PEM protein was determined similarly to that for the yeast two-hybrid proteins, except that lysates were prepared from 7 OD units of cells, and anti-GFP antibodies were used.

Microscopy

For live-cell microscopy, cells carrying constructs for expression of fluorescently tagged proteins were grown to mid log phase in appropriate media. Fluorescence microscopy observation was carried out using a deconvolution Axioscope microscope (Carl Zeiss,

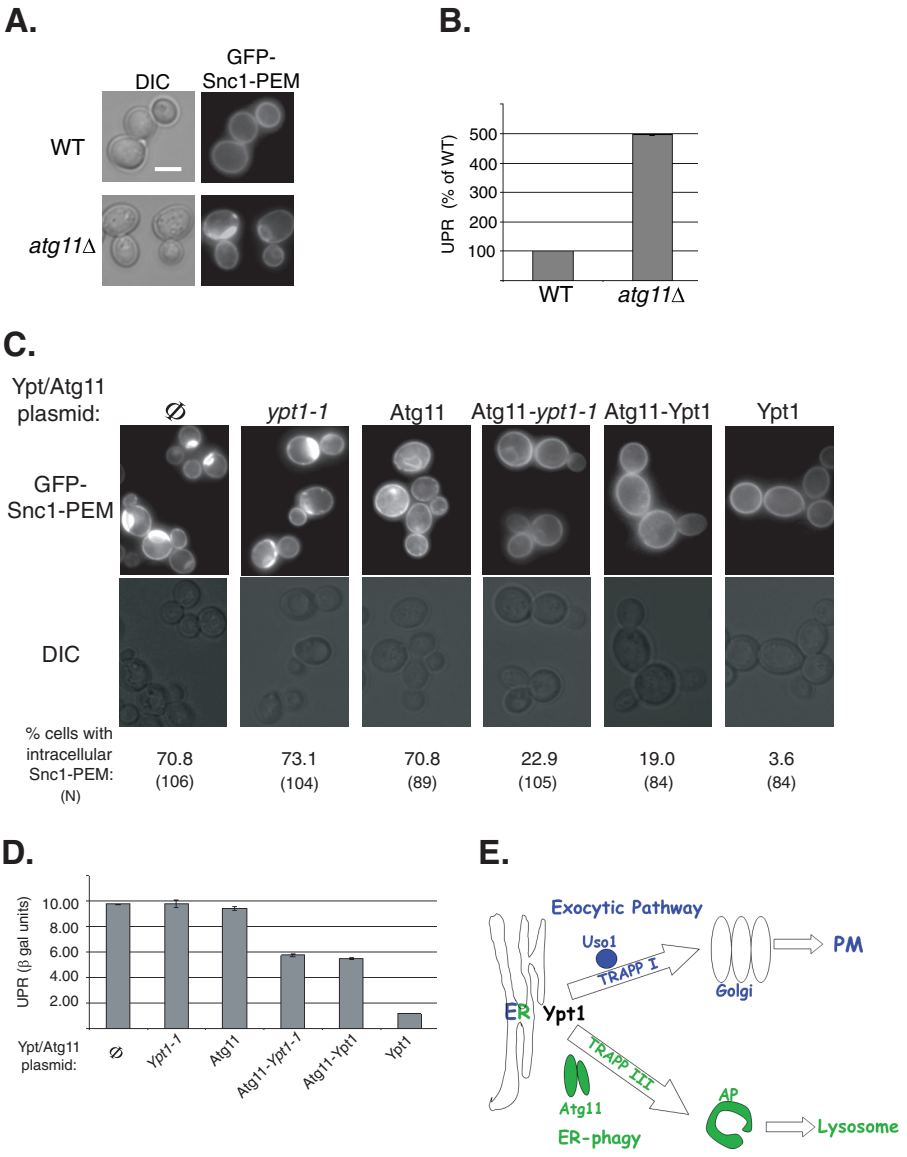

FIGURE 10: A role for the Ypt1-Atg11 interaction in ER phagy. (A) GFP-Snc1-PEM accumulates in *atg11Δ* mutant cells. Wild-type and *atg11Δ* mutant cells expressing GFP-Snc1-PEM were visualized by live-cell microscopy. Representative cells are shown (25 cells for each strain), DIC (left) and GFP (right). (B) UPR is induced in *atg11Δ* mutant cells expressing GFP-Snc1. UPR was determined in wild-type and *atg11Δ* mutant cells expressing GFP-Snc1 and LacZ under a UPR-inducible promoter as in Figure 8. (C) The Atg11-Ypt1-T40K fusion protein complements the GFP-Snc1-PEM accumulation defect of *ypt1-1* mutant cells. *Ypt1-1* mutant cells expressing GFP-Snc1-PEM were transformed with a *CEN* plasmid to express the following proteins (left to right): Φ, empty vector control, Ypt1-1, Atg11, Atg11-Ypt1-T40K, Atg11-Ypt1, and Ypt1. Cells were visualized by live-cell microscopy, and representative cells are shown (GFP, top; DIC, bottom). Percentage of cells with intracellular GFP-Snc1-PEM is indicated at the bottom (*N*, number of cells visualized). Approximately 70% of *ypt1-1* mutant cells accumulate intracellular GFP-Snc1-PEM (Φ, left). This defect can be suppressed by Ypt1 (right), as well as by the two fusion proteins, Atg11-Ypt1-T40K and Atg11-Ypt1, but not by Ypt1-T40K or Atg11 proteins. (D) Suppression of UPR induction in *ypt1-1* mutant cells by the Atg11-Ypt1-T40K fusion protein. *Ypt1-1* mutant cells were transformed with two plasmids expressing LacZ under a UPR-inducible promoter and Atg11/Ypt1. Induction of the UPR was determined using the βGAL assay. UPR is induced in *ypt1-1* mutant cells (Φ, left, and this induction is suppressed by overexpression of Ypt1 (right), as well as by the two fusion proteins, Atg11-Ypt1-T40K and Atg11-Ypt1, but not by Ypt1-T40K or Atg11 proteins. Bar, 5 μm; error bars, SD (B, D). Results shown in A–D represent at least two independent experiments. (E) Model depicting a role for Ypt1, together with its process-specific GEFs and effectors, in coordinating ER-to-Golgi and ER-phagy. Here we show that, whereas in wild-type cells some overexpressed GFP-tagged Snc1 is transported from the ER to the PM via the exocytic pathway, some is shuttled to the lysosome (vacuole in yeast) for degradation through the autophagic pathway. Ypt1 is required for both pathways. In the exocytic pathway Ypt1 is activated by TRAPP I and mediates ER-to-Golgi transport via vesicles; Uso1/p115 is an example of an ER-to-Golgi–specific effector (Cao *et al.*, 1998; Allan *et al.*, 2000). In autophagy, Ypt1 is activated by Trs85-containing TRAPP III to shuttle ER-derived membranes loaded with misfolded proteins to autophagosomes; Atg11 is an autophagy-specific effector (Lipatova *et al.*, 2012). In *ypt1-1*, *trs85Δ*, and *atg11Δ* mutant cells, shuttling of GFP-Snc1 from the ER to the autophagosome is defective, GFP-Snc1 accumulates in aberrant ER structures, and the ER-stress response, UPR, is induced.

Thornwood, NY) with fluorescein isothiocyanate (GFP and YFP) and Texas red (mCherry) sets of filters. Labeling of endosome and vacuole membranes with FM4-64 was done using a 5-min pulse and 5- and 60-min chases, respectively, as previously described (Vida and Emr, 1995). Immuno–electron microscopy was done as previously described (Preuss *et al.*, 1992).

UPR βgal assay

The βgal assay was done with cells transformed with a plasmid (pJC104) encoding the lacZ gene behind four repeats of a UPR element (Kruse *et al.*, 2006). To induce UPR, cells were grown in the presence of 5 μg/ml tunicamycin for 90 min. The level of β-galactosidase in cell lysates was determined as previously described (Reynolds *et al.*, 2001). To prepare cell lysates, 5 OD_{600} units of early-log-phase cells were spun down, washed in distilled H_2O + 2 mM phenylmethylsulfonyl fluoride, resuspended in 100 μl of lysis buffer (20 mM 1,4-piperazinediethanesulfonic acid, pH 7.0, 0.5% Triton X-100, 50 mM KCl, 100 mM potassium acetate, 10 mM $MgSO_4$, 1 mM DTT, protease inhibitors), and vortexed with glass beads. The resulting lysate was transferred to a fresh Eppendorf tube, the beads were vortexed with additional 200 μl of lysis buffer, and the lysate was combined with the previous one. One volume of the lysate was combined with nine volumes of Z buffer (60 mM Na_2HPO_4, 40 mM NaH_2PO_4, 10 mM KCl, 1 mM $MgSO_4$, 50 mM β-mercaptoethanol, pH 7.0) and allowed to equilibrate at 28°C for 15 min. On addition of 4 mg/ml *o*-nitrophenyl-β-D-galactoside, timing was started. When the solution turned yellow, 1 M Na_2CO_3 was added to terminate the reaction.

ACKNOWLEDGMENTS

We thank J. Goeckeler and J. Brodsky for the UPR plasmid, R. Wright for anti-Hmg1 antibody, D. Klionsky for anti-Ape1, X. Zhang for technical help, and D. Taussig for critical reading of the manuscript. This research was supported by National Institutes of Health Grant GM-45444 to N.S.

REFERENCES

Allan BB, Moyer BD, Balch WE (2000). Rab1 recruitment of p115 into a cis-SNARE complex: programming budding COPII vesicles for fusion. Science 289, 444–448.

Bernales S, Schuck S, Walter P (2007). ER-phagy: selective autophagy of the endoplasmic reticulum. Autophagy 3, 285–287.

Cai Y *et al*. (2008). The structural basis for activation of the Rab Ypt1p by the TRAPP membrane-tethering complexes. Cell 133, 1202–1213.

Cao X, Ballew N, Barlowe C (1998). Initial docking of ER-derived vesicles requires Uso1p and Ypt1p but is independent of SNARE proteins. EMBO J 17, 2156–2165.

Chen SH, Chen S, Tokarev AA, Liu F, Jedd G, Segev N (2005). Ypt31/32 GTPases and their novel F-box effector protein Rcy1 regulate protein recycling. Mol Biol Cell 16, 178–192.

Cheong H, Klionsky DJ (2008). Biochemical methods to monitor autophagy-related processes in yeast. Methods Enzymol 451, 1–26.

Choi AM, Ryter SW, Levine B (2013). Autophagy in human health and disease. N Engl J Med 368, 651–662.

Chua CE, Gan BQ, Tang BL (2011). Involvement of members of the Rab family and related small GTPases in autophagosome formation and maturation. Cell Mol Life Sci 68, 3349–3358.

Deegan S, Saveljeva S, Gorman AM, Samali A (2013). Stress-induced self-cannibalism: on the regulation of autophagy by endoplasmic reticulum stress. Cell Mol Life Sci 70, 2425–2441.

Fantini J, Yahi N (2010). Molecular insights into amyloid regulation by membrane cholesterol and sphingolipids: common mechanisms in neurodegenerative diseases. Expert Rev Mol Med 12, e27.

Franzusoff A, Redding K, Crosby J, Fuller RS, Schekman R (1991). Localization of components involved in protein transport and processing through the yeast Golgi apparatus. J Cell Biol 112, 27–37.

He C, Klionsky DJ (2009). Regulation mechanisms and signaling pathways of autophagy. Annu Rev Genet 43, 67–93.

Howell GJ, Holloway ZG, Cobbold C, Monaco AP, Ponnambalam S (2006). Cell biology of membrane trafficking in human disease. Int Rev Cytol 252, 1–69.

Huh WK, Falvo JV, Gerke LC, Carroll AS, Howson RW, Weissman JS, O'Shea EK (2003). Global analysis of protein localization in budding yeast. Nature 425, 686–691.

Jedd G, Mulholland J, Segev N (1997). Two new Ypt GTPases are required for exit from the yeast *trans*-Golgi compartment. J Cell Biol 137, 563–580.

Jedd G, Richardson C, Litt R, Segev N (1995). The Ypt1 GTPase is essential for the first two steps of the yeast secretory pathway. J Cell Biol 131, 583–590.

Jones EW, Zubenko GS, Parker RR (1982). PEP4 gene function is required for expression of several vacuolar hydrolases in *Saccharomyces cerevisiae*. Genetics 102, 665–677.

Jones S, Jedd G, Kahn RA, Franzusoff A, Bartolini F, Segev N (1999). Genetic interactions in yeast between Ypt GTPases and Arf guanine nucleotide exchangers. Genetics 152, 1543–1556.

Jones S, Newman C, Liu F, Segev N (2000). The TRAPP complex is a nucleotide exchanger for Ypt1 and Ypt31/32. Mol Biol Cell 11, 4403–4411.

Kim J, Kamada Y, Stromhaug PE, Guan J, Hefner-Gravink A, Baba M, Scott SV, Ohsumi Y, Dunn WA Jr, Klionsky DJ (2001). Cvt9/Gsa9 functions in sequestering selective cytosolic cargo destined for the vacuole. J Cell Biol 153, 381–396.

Kruse KB, Brodsky JL, McCracken AA (2006). Characterization of an ERAD gene as VPS30/ATG6 reveals two alternative and functionally distinct protein quality control pathways: one for soluble Z variant of human alpha-1 proteinase inhibitor (A1PiZ) and another for aggregates of A1PiZ. Mol Biol Cell 17, 203–212.

Lewis MJ, Nichols BJ, Prescianotto-Baschong C, Riezman H, Pelham HR (2000). Specific retrieval of the exocytic SNARE Snc1p from early yeast endosomes. Mol Biol Cell 11, 23–38.

Lipatova Z, Belogortseva N, Zhang XQ, Kim J, Taussig D, Segev N (2012). Regulation of selective autophagy onset by a Ypt/Rab GTPase module. Proc Natl Acad Sci USA 109, 6981–6986.

Lynch-Day MA, Bhandari D, Menon S, Huang J, Cai H, Bartholomew CR, Brumell JH, Ferro-Novick S, Klionsky DJ (2010). Trs85 directs a Ypt1 GEF, TRAPPIII, to the phagophore to promote autophagy. Proc Natl Acad Sci USA 107, 7811–7816.

Meiling-Wesse K, Epple UD, Krick R, Barth H, Appelles A, Voss C, Eskelinen EL, Thumm M (2005). Trs85 (Gsg1), a component of the TRAPP complexes, is required for the organization of the preautophagosomal structure during selective autophagy via the CVT pathway. J Biol Chem 280, 33669–33678.

Morozova N, Liang Y, Tokarev AA, Chen SH, Cox R, Andrejic J, Lipatova Z, Sciorra VA, Emr SD, Segev N (2006). TRAPPII subunits are required for the specificity switch of a Ypt-Rab GEF. Nat Cell Biol 8, 1263–1269.

Nakatogawa H, Suzuki K, Kamada Y, Ohsumi Y (2009). Dynamics and diversity in autophagy mechanisms: lessons from yeast. Nat Rev 10, 458–467.

Nazarko TY, Huang J, Nicaud JM, Klionsky DJ, Sibirny AA (2005). Trs85 is required for macroautophagy, pexophagy and cytoplasm to vacuole targeting in *Yarrowia lipolytica* and *Saccharomyces cerevisiae*. Autophagy 1, 37–45.

Preuss D, Mulholland J, Franzusoff A, Segev N, Botstein D (1992). Characterization of the *Saccharomyces* Golgi complex through the cell cycle by immunoelectron microscopy. Mol Biol Cell 3, 789–803.

Preuss D, Mulholland J, Kaiser CA, Orlean P, Albright C, Rose MD, Robbins PW, Botstein D (1991). Structure of the yeast endoplasmic reticulum: localization of ER proteins using immunofluorescence and immunoelectron microscopy. Yeast 7, 891–911.

Reynolds A, Lundblad V, Dorris D, Keaveney M (2001). Yeast vectors and assays for expression of cloned genes. Curr Protoc Mol Biol Chapter 13, Unit 13.6.

Rubinsztein DC, Shpilka T, Elazar Z (2012). Mechanisms of autophagosome biogenesis. Curr Biol 22, R29–R34.

Sacher M, Barrowman J, Wang W, Horecka J, Zhang Y, Pypaert M, Ferro-Novick S (2001). TRAPP I implicated in the specificity of tethering in ER-to-Golgi transport. Mol Cell 7, 433–442.

Sacher M, Jiang Y, Barrowman J, Scarpa A, Burston J, Zhang L, Schieltz D, Yates JR3rd, Abeliovich H, Ferro-Novick S (1998). TRAPP, a highly conserved novel complex on the *cis*-Golgi that mediates vesicle docking and fusion. EMBO J 17, 2494–2503.

Schroder M (2008). Endoplasmic reticulum stress responses. Cell Mol Life Sci 65, 862–894.

Sclafani A, Chen S, Rivera-Molina F, Reinisch K, Novick P, Ferro-Novick S (2010). Establishing a role for the GTPase Ypt1p at the late Golgi. Traffic 11, 520–532.

Segev N (1991). Mediation of the attachment or fusion step in vesicular transport by the GTP-binding Ypt1 protein. Science 252, 1553–1556.

Segev N (2001a). Ypt and Rab GTPases: insight into functions through novel interactions. Curr Opin Cell Biol 13, 500–511.

Segev N (2001b). Ypt/Rab GTPases: regulators of protein trafficking. Sci STKE 2001, re11.

Segev N (2011). Coordination of intracellular transport steps by GTPases. Semin Cell Dev Biol 22, 33–38.

Segev N, Botstein D (1987). The ras-like yeast YPT1 gene is itself essential for growth, sporulation, and starvation response. Mol Cell Biol 7, 2367–2377.

Segev N, Mulholland J, Botstein D (1988). The yeast GTP-binding YPT1 protein and a mammalian counterpart are associated with the secretion machinery. Cell 52, 915–924.

Stenmark H (2009). Rab GTPases as coordinators of vesicle traffic. Nat Rev 10, 513–525.

Tooze SA, Yoshimori T (2010). The origin of the autophagosomal membrane. Nat Cell Biol 12, 831–835.

Uversky VN, Oldfield CJ, Midic U, Xie H, Xue B, Vucetic S, Iakoucheva LM, Obradovic Z, Dunker AK (2009). Unfoldomics of human diseases: linking protein intrinsic disorder with diseases. BMC Genomics 10 (Suppl 1), S7.

Vembar SS, Brodsky JL (2008). One step at a time: endoplasmic reticulum-associated degradation. Nat Rev 9, 944–957.

Vida TA, Emr SD (1995). A new vital stain for visualizing vacuolar membrane dynamics and endocytosis in yeast. J Cell Biol 128, 779–792.

Wach A, Brachat A, Alberti-Segui C, Rebischung C, Philippsen P (1997). Heterologous HIS3 marker and GFP reporter modules for PCR-targeting in *Saccharomyces cerevisiae*. Yeast 13, 1065–1075.

Wang RC, Levine B (2010). Autophagy in cellular growth control. FEBS Lett 584, 1417–1426.

Wang W, Sacher M, Ferro-Novick S (2000). TRAPP stimulates guanine nucleotide exchange on Ypt1p. J Cell Biol 151, 289–296.

Yang Z, Klionsky DJ (2009). An overview of the molecular mechanism of autophagy. Curr Top Microbiol Immunol 335, 1–32.

Zou S, Liu Y, Zhang XQ, Chen Y, Ye M, Zhu X, Yang S, Lipatova Z, Liang Y, Segev N (2012). Modular TRAPP complexes regulate intracellular protein trafficking through multiple Ypt/Rab GTPases in *Saccharomyces cerevisiae*. Genetics 191, 451–460.